Molecular Dynamics Simulations Reveal Isoform Specific Contact Dynamics between the Plexin Rho GTPase Binding Domain (RBD) and Small Rho GTPases Rac1 and Rnd1

Liqun Zhang*[1], and Matthias Buck*[2-6]

[1]Tennessee Technological University, Chemical Engineering Department, 1 William L Jones Dr., Cookeville, Tennessee 38505, United States.

[2]Department of Physiology and Biophysics, Medical School of Case Western Reserve University, Cleveland, Ohio 44106, United States.

[3]Department of Neurosciences, [4]Department of Pharmacology, [5]Case Comprehensive Cancer Center as well as [6]Center for Proteomics and Bioinformatics, Case Western Reserve University, School of Medicine, 10900 Euclid Avenue, Cleveland, Ohio 44106, United States of America

Supplemental Information

1. **Tables:**

Table S1. Amino acid sequences of proteins used in the simulations

1. Plexin-B1 RBD

[6] [34]

*****YRPLTLNALLAVGPGAGEAQGVPVKVLDCDTISQAKEKMLDQLYKGVPLTQRPDPRTLDVEWRSGVAGHLI
LSDEDVTSEVQGLFRRLNTLQHYKVPDGATVALVPCLT*

2. Plexin-B1 RBD + RAC1 complex, in HSD and HSP state

[6] [34]

*****YRPLTLNALLAVGPGAGEAQGVPVKVLDCDTISQAKEKMLDQLYKGVPLTQRPDPRTLDVEWRSGVAGHLI
LSDEDVTSEVQGLWRRLNTLQHYKVPDGATVALVPCLT/M
QAIKCVVVGDGAVGKTCLLISYTTNAFPGEYIPTVFDNYSANVMVDGKPVNLGLWDTAGQEDYDRLRPLSYPQTDV
FLICFSLVSPASFENVRAKWYPEVRHHCPNTPIILVGTKLDLRDDKDTIEKLKEKKLTPITYPQGLAMAKEIGAVK
YLECSALTQRGLKTVFDEAIRAVLK

3. plexin-B1 RBD + RND1 complex, in HSD and HSP state

[6] [34]

*****YRPLTLNALLAVGPGAGEAQGVPVKVLDCDTISQAKEKMLDQLYKGVPLTQRPDPRTLDVEWRSGVAGHLI
LSDEDVTSEVQGLWRRLNTLQHYKVPDGATVALVPC/******PQP
VVARCKLVLVGDVQCGKTAMLQVLAKDCYPETYVPTVFENYTACLETEEQRVELSLWDTSGSPYYDNVRPLCYSDS
DAVLLCFDISRPETVDSALKKWRTEILDYCPSTRVLLIGCKTDLRTDLSTLMELSHQKQAPISYEQGCAIAKQLGA
EIYLEGSAFTSEKSIHSIFRTASMLCL

4. Plexin-A1 RBD

[9] [34]

********YKTLTLNCVN**PEHENAPE**VPVKGLN**C**DTVTQVKEKLLDAVYKGVPYSQRPKAGDMDLEWR**QGRMA**RII
LQDEDVTTKIDNDWKRLNTLAHYQVTDGSSVALVPKQ*

5. plexin-A1 RBD + RAC1 complex, in HSD and HSP state
[9] [34]
********YKTLTLNCVN**PEHENAPE**VPVKGLN**C**DTVTQVKEKLLDAVYKGVPYSQRPKAGDMDLEWR**QGRMA**RII
LQDEDVTTKIDNDWKRLNTLAHYQVTDGSSVALVPKQ/*
QAIKCVVVGDGAVGKTCLLISYTTNA**FPGEYIPTVFDNYSANV**M**VDGK**PVNLGLWDTAG**LEDYDRLRPLSYPQTD**V
FLICFSLVSPASFENVRAKWYPEVRHHCPNTPIILVGTKLDLRDDKDTIEKLKEKKLTPITYPQGLAMAKEIGAVK
YLECSALTQRGLKTVFDEAIRAV

6. Plexin-A2 RBD
[2] [34]
*LIRQQIEYKTLILNCVN**PDNENSPE**IPVKVLN**C**DTITQVKEKILDAVYKNVPYSQRPRAVDMDLEWR**QGRIA**RVV
LQDEDITTKIEGDWKRLNTLMHYQVSDRSVVALVPK*

7. Plexin-A2 RBD + RND1 Complex, in HSD and HSP state
[2] [34]
*LIRQQIEYKTLILNCVN**PDNENSPE**IPVKVLN**C**DTITQVKEKILDAVYKNVPYSQRPRAVDMDLEWR**QGRIA**RVV
LQDEDITTKIEGDWKRLNTLMHYQVSDRSVVALVPK/**********RCKLVLVGDVQCGKTAMLQVLAKDC**YP**
ETYVPTVFENYTACLE**TEEQ**RVELSLWDTSG**SPYYDNVRPLCYSDSD**AVLLCFDISRPETVDSALKKWRTEILDYC
PSTRVLLIGCKTDLRTDLSTLMELSHQKQAPISYEQGCAIAKQLGAEIYLEGSAFTSEKSI.SIFRTASMLCLN

8. RAC1 GTPase
*QAIKCVVVGDGAVGKTCLLISYTTNA**FPGEYIPTVFDNYSANV**M**VDGK**PVNLGLWDTAG**QEDYDRLRPLSYPQTD**
VSLICFSLVSPASFENVRAKWYPEVRHHCPNTPIILVGTKLDLRDDKDTIEKLKEKKLTPITYPQGLAMAKEIGAV
KYLECSALTQRGLKTVFDEAIRAVLCP

9. RND1 GTPase
*********VVARCKLVLVGDVQCGKTAMLQVLAKDC**YPETYVPTVFENYTACL**E**TEEQ**RVELSLWDTSG**SPYYDN**
VRPLCYSDSDAVLLCFDISRPETVDSALKKWRTEILDYCPSTRVLLIGCKTDLRTDLSTLMELSHQKQAPISYEQG
CAIAKQLGAEIYLEGSAFTSEKSIHSIFRTASMLCL

In above table, the RBD residues shown in bold red and underlined are for the L1, L3 and L4 loop regions respectively; the residues shown in bold blue and underlined are for the Rac1/Rnd1 SW I, inter-switch(β2-3) and SW II regions. The residues shown in bold green are the extra residues, not seen in the crystal structures. For all RBDs the Cysteine residue in the turn between β-strand 2 and α-helix 1 was labelled with residue 34 as the reference. Both this Cysteine residue as well as the domain starting residue are labelled and colored in Magenta. * does not represent actual residues, but was put there for alignment.

Table S2: Overview of simulation run length, number of atoms and box size

Simulation	Simulation time (ns)	Number of atoms	Box size ($Å^3$)
Complexes:			
RBD-B1: Rnd1, HSD	1000	85248	112.2 x 99.8 x 91.4
RBD-B1: Rnd1, HSP	1000	85721	112.3 x 99.8 x 92.0
RBD-B1: Rac1, HSD	2400	80689	112.9 x 97.2 x 89.1
RBD-B1: Rac1, HSP	2400	95345	112.8 x 114.2 x 113.4
RBD-A1: Rac1, HSD	1000	76345	113.8 x 95.3 x 86.1
RBD-A1: Rac1, HSP	1000	76402	112.1 x 95.3 x 85.9
RBD-A2: Rnd1, HSD	1000	77621	107.4 x 98.2 x 85.0
RBD-A2: Rnd1, HSP	1000	77645	107.4 x 98.2 x 85.0
Free Proteins:			
Rac1	1000	63808	95.3 x 88.1 x 82.9
Rnd1	1000	66325	100.4 x 86.0 x 83.5
RBD-A1	1000	56746	94.2 x 82.1 x 80.3
RBD-A2	1000	53995	91.1 x 81.1 x 80.2
RBD-B1	1000	46598	86.4 x 78.1 x 75.5
RBD-B1-s	2400	52656	90.0 x 84.3 x 75.8

Table S3: Mainchain RMSD relative to the starting structures (average over last 500 ns with ± as standard deviation)

Simulation	RBD (Å)	GTPase (Å)	Complex (Å)
Complexes:			
RBD-B1: Rnd1, HSD	2.3 ± 0.3	1.5 ± 0.1	2.9 ± 0.3
RBD-B1: Rnd1, HSP	4.6 ± 0.3	1.6 ± 0.1	5.1 ± 0.2
RBD-B1: Rac1, HSD	3.0 ± 0.2	2.3 ± 0.2	4.9 ± 0.2
RBD-B1: Rac1, HSP	3.3 ± 0.2	1.8 ± 0.2	4.9 ± 0.3
RBD-A1: Rac1, HSD	3.8 ± 0.2	1.6 ± 0.1	4.6 ± 0.3
RBD-A1: Rac1, HSP	3.4 ± 0.2	1.3 ± 0.1	3.1 ± 0.5
RBD-A2: Rnd1, HSD	3.1 ± 0.3	1.8 ± 0.2	2.8 ± 0.2
RBD-A2: Rnd1, HSP	3.8 ± 0.1	2.2 ± 0.3	3.7 ± 0.2
Free Proteins:			
Rac1		1.3 ± 0.1	
Rnd1		1.5 ± 0.2	
RBD-A1	2.5 ± 0.2		
RBD-A2	4.4 ± 0.5		
RBD-B1	4.0 ± 0.2		

Table S4. Residues forming contacts on the binding interface of the RBD-B1 : Rac1 GTPase complex in the HSD state. Only resdue pairs forming contacts with occupancy ratio higher than 5% are shown. The residue pairs having the occupancy ratio higher than 30% are highlighted in red, only higher than 20% in blue. * marks residues observed in contact in the starting coordinates derived from the X-ray structures.

RBD-B1	Rac1	Occupancy(%)	Ligplot/Dimplot
ARG68-Main	ASN39-Side	9.2%	
SER69-Side	PHE37-Main	17.1%	*
SER69-Side	ASP38-Side	6.1%	
SER69-Side	ASN39-Side	5.2%	
GLY70-Main	ASN39-Side	23.7%	
GLY70-Main	ASN39-Side	14.2%	
GLY70-Main	SER71-Side	13.2%	
VAL71-Main	VAL36-Main	9.3%	
VAL71-Main	SER71-Side	5.1%	
ALA72-Main	SER71-Side	5.3%	
GLY73-Main	LYS5-Side	14.1%	
HSD74-Side	ASN39-Side	9.5%	*
ASP81-Side	ARG66-Side	72.2%	
THR83-Side	ARG66-Side	6.7%	*
GLU85-Side	ARG66-Side	23.0%	*
ASN94-Side	ARG66-Side	14.3%	
HSD98-Side	ARG66-Side	28.6%	*
LYS100-Side	ASP63-Side	42.5%	*
LYS100-Main	TYR64-Side	40.0%	
LYS100-Side	ASP63-Main	18.0%	*
THR106-Side	ASP38-Side	15.2%	

Table S5. Residues forming contacts on the binding interface of the RBD-B1 : Rac1 GTPase complex in the HSP state. Only residue pairs forming contacts with occupancy ratio higher than 5% are shown. The residue pairs having the occupancy ratio higher than 30% are highlighted in red, only higher than 20% in blue.

RBD-B1	RAC1	Occupancy(%)	Ligplot/Dimplot
GLY73-Main	ASP38-Side	54.1%	
HSP74-Side	ASN39-Side	8.5%	*
ILE76-Main	LEU70-Main	13.2%	*
ASP81-Side	HSP104-Side	13.1%	
THR83-Side	HSP104-Side	5.4%	
THR83-Main	CYS105-Main	5.8%	
HSP98-Main	ARG66-Side	9.0%	*
TYR99-Main	ARG66-Side	7.7%	
LYS100-Side	ASP63-Side	11.9%	*
LYS100-Main	ARG66-Side	5.8%	
LEU113-Main	GLN74-Side	10.8%	
THR114-Side	MET1-Main	14.9%	
THR114-Side	GLN2-Main	7.9%	

Table S6. Residues forming contacts on the binding interface of the RBD-A1 : Rac1 GTPase complex in the HSD state. Only residue pairs forming contacts with occupancy ratio higher than 5% are shown. The residue pairs having the occupancy ratio higher than 30% are highlighted in red, only higher than 20% in blue.

RBD-A1	RAC1	Occupancy (%)	Ligplot/Dimplot
GLN69-Side	THR35-Side	10.5%	
GLN69-Side	VAL36-Main	19.7%	
GLN69-Side	PHE37-Main	9.6%	*
GLN69-Side	TYR64-Side	10.8%	
ALA73-Side	THR35-Side	6.4%	
GLN78-Side	ARG66-Side	13.2%	
ASP79-Side	ARG66-Side	36.1%	
THR83-Side	ARG66-Side	9.1%	
LYS85-Side	ASP65-Side	23.1%	
LYS85-Side	GLU100-Side	21.6%	
ASP87-Side	ARG66-Side	22.5%	
ARG92-Side	GLU62-Side	27.4%	
ARG92-Side	GLU62-Main	24.4%	
LEU93-Main	ARG66-Side	13.9%	
HSD98-Side	ARG66-Side	38.9%	
GLN100-Side	ASP63-Main	12.4%	
GLN100-Side	ASP63-Side	14.9%	

Table S7. Residues forming contacts on the binding interface of the RBD-A1 : Rac1 GTPase complex in HSP state. Only residue pairs forming contacts with occupancy ratio higher than 5% are shown. The residue pairs having the occupancy ratio higher than 30% are highlighted in red, only higher than 20% in blue.

RBD-A1	RAC1	Occupancy (%)	Ligplot/Dimplot
GLN69-Side	THR35-Side	13.8%	
GLN69-Side	VAL36-Main	25.0%	
ARG71-Side	GLU31-Side	12.5%	
ARG71-Side	ASP38-Side	43.8%	*
ARG71-Side	ASN39-Main	32.3%	
ASP81-Side	ARG66-Side	6.5%	
THR84-Side	HSP104-Side	6.2%	
THR84-Main	HSP104-Side	28.7%	
LYS85-Side	GLU62-Side	15.6%	
LYS85-Side	GLU100-Side	60.7%	
LYS85-Main	HSP103-Side	33.7%	
ASP87-Side	ARG102-Side	60.0%	
ASP87-Side	HSP103-Side	65.3%	
ARG92-Side	ASP65-Side	12.0%	
LEU93-Main	ARG66-Side	53.8%	
ASN94-Side	ARG66-Side	87.4%	
GLN100-Side	ASP63-Main	20.3%	

GLN100-Side	ASP63-Side	6.6%	

Table S8. Residues forming contacts on the binding interface of the RBD-A2 : Rnd1 GTPase complex in the HSD state. Only residue pairs forming contacts with occupancy ratio higher than 5% are shown. The residue pairs having the occupancy ratio higher than 30% are highlighted in red, only higher than 20% in blue.

RBD-A2	RND1	Occupancy(%)	Ligplot/Dimplot
LEU2-Main	ASP75-Side	5.0%	
ILE3-Main	PRO72-Main	6.2%	
ILE3-Main	TYR73-Side	14.5%	
GLN5-Side	TYR73-Main	6.3%	
GLN5-Side	TYR74-Side	5.7%	
GLN69-Side	PHE47-Side	5.5%	*
GLN69-Side	PHE47-Main	5.1%	*
ARG71-Side	GLU48-Side	13.4%	
ARG71-Main	GLU48-Side	12.0%	
ARG71-Side	ASN49-Main	10.0%	
THR83-Main	PRO79-Side	5.5%	
THR84-Side	ASN76-Side	8.0%	
LYS85-Side	ASP75-Side	72.9%	
LYS85-Main	ASN76-Side	5.4%	
LYS85-Main	ASN76-Side	54.2%	
LYS85-Side	GLU110-Side	62.0%	
LYS85-Side	ASP113-Side	13.6%	
LYS85-Main	TYR114-Side	7.4%	
TRP90-Side	ASN76-Side	5.5%	
HSD98-Main	ASN76-Side	88.0%	*
HSD98-Side	ASN76-Side	25.4%	*
GLN100-Side	TYR73-Main	19.8%	
GLN100-Side	ASP75-Main	55.6%	
GLN100-Side	PRO72-Main	11.6%	
GLN100-Main	TYR74-Side	6.8%	*
GLN100-Side	ASN76-Side	8.7%	
GLN100-Side	ASN76-Main	90.0%	
SER102-Side	TYR74-Side	23.4%	
SER102-Side	TYR74-Side	14.6%	

Table S9. Residues forming contacts on the binding interface of the RBD-A2 : Rnd1 GTPase complex in HSP state. Only residue pairs forming contacts with occupancy ratio higher than 5% are shown. The residue pairs having the occupancy ratio higher than 30% are highlighted in red, only higher than 20% in blue.

RBD-A2	RND1	Occupancy (%)	Ligplot/Dimplot
ILE3-Main	SER71-Side	42.0%	
ARG4-Side	TYR73-Main	25.5%	
ARG4-Side	ASP75-Side	11.8%	
GLN6-Main	TYR74-Side	8.7%	
GLN6-Side	TYR74-Side	6.1%	
GLN69-Side	THR45-Side	16.1%	
GLN69-Side	VAL46-Side	8.0%	
GLN69-Side	VAL46-Main	5.4%	
ARG71-Side	GLU40-Side	10.3%	
ARG71-Side	GLU48-Side	27.7%	
ARG71-Side	ASN49-Main	10.7%	
ILE72-Side	ASN49-Main	6.9%	
GLN78-Side	SER83-Side	14.6%	
ARG92-Side	ASN76-Side	84.9%	
ARG92-Side	TYR114-Side	18.9%	
HSP98-Side	ASP75-Side	78.5%	
HSP98-Main	ASN76-Main	11.6%	*
GLN100-Side	TYR74-Side	7.7%	*
GLN100-Side	ASN76-Side	10.4%	

Table S10. Residues forming contacts on the binding interface of the RBD-B1 : Rnd1 GTPase complex in the HSD state. Only residue pairs forming contacts with occupancy ratio higher than 5% are shown. The residue pairs having the occupancy ratio higher than 30% are highlighted in red, only higher than 20% in blue.

RBD-B1	RND1	Occupancy (%)	Ligplot/Dimplot
TRP67-Main	PHE47-Side	10.2%	*
TRP67-Side	PHE47-Side	13.7%	*
SER69-Side	THR45-Side	8.1%	
SER69-Side	VAL46-Main	7.4%	
SER69-Side	PHE47-Main	11.6%	*
GLY70-Main	GLU48-Side	20.2%	*
ALA72-Main	GLU48-Side	59.3%	*
ALA72-Main	ASN49-Side	11.1%	*
ALA72-Side	ASN49-Main	7.2%	
GLY73-Main	ASN49-Side	6.9%	
HSD74-Main	ASN49-Side	19.5%	
HSD74-Main	TRP66-Side	32.6%	*
LEU75-Side	TRP66-Side	6.7%	
VAL82-Side	PRO79-Main	5.7%	
VAL82-Side	SER83-Side	6.8%	
THR83-Side	ASP113-Main	8.6%	
THR83-Side	TYR114-Main	22.2%	
HSD98-Side	ASN76-Side	10.4%	*
HSD98-Main	ASN76-Side	53.9%	*
HSD98-Side	ASN76-Side	14.3%	
TYR99-Side	ASN76-Main	7.3%	*
TYR99-Main	VAL77-Side	15.7%	
TYR99-Side	LEU80-Side	12.2%	
LYS100-Side	TYR73-Main	29.6%	*
LYS100-Main	TYR74-Side	5.5%	*
LYS100-Side	ASP75-Side	11.5%	
LYS100-Side	ASN76-Side	10.7%	

Table S11. Residues forming contacts on the binding interface of the RBD-B1 : Rnd1 GTPase complex in the HSD state. Only residue pairs forming contacts with occupancy ratio higher than 5% are shown. The residue pairs having the occupancy ratio higher than 30% are highlighted in red, only higher than 20% in blue.

RBD-B1	RND1	Occupancy (%)	Ligplot/Dimplot
SER69-Side	VAL46-Side	7.8%	
SER69-Side	TYR74-Side	32.1%	
ALA72-Main	ASN49-Main	11.3%	*
GLY73-Main	PHE47-Main	8.5%	*
GLY73-Main	ASN49-Side	28.7%	
HSP74-Main	ASN49-Side	26.8%	
HSP74-Main	ASN49-Side	93.9%	
HSP74-Side	ASN49-Side	34.6%	
LEU75-Side	TRP66-Side	9.9%	
ASP81-Side	SER83-Side	29.4%	
ASP81-Side	TYR114-Side	9.4%	
THR83-Side	TYR114-Main	8.5%	
ARG92-Side	ASP84-Side	5.6%	
HSP98-Side	TYR114-Side	11.7%	
TYR99-Side	LEU80-Sid	6.4%	
TYR99-Main	LEU80-Side	5.9%	
TYR99-Main	PRO79-Side	8.9%	
LYS100-Main	ASN76-Side	57.3%	
LYS100-Side	ASP75-Side	49.4%	
LYS100-Side	ASP75-Main	7.7%	

Supplementary Text for Tables S4-11:

For RBD-A2 : Rnd1 complexes in the HSD state, the RBD residues on the binding interface include the residues from residue 2 to 5, then from residue 62 to 102. The RBD β1, β3, L3 loop, β4, L4 loop, α2 helix segements are involved in the binding. In the HSP form, the binding interface residues include residues from residues 2 to 5, then from residue 68 to 99. Thus the same regions are involved in the binding in both forms. There is one HSP residues in the RBD of plexinA2, which is HSP98 and which is located at the binding interface. For Rnd1, mostly β2 and β3, and α3 comprise the binding interface. There are two HSP residues in Rnd1. One is HSP144, the other is HSP177, but these are far from the binding interface. In the HSP form, Rnd1 helix α2 is also at the binding interface. Checking the most persistent residue contact pairs in the HSD form, HSD98 (in RBD-A2) and Asn76 (in Rnd1) are bound for 88% of the time. Lys85 (on RBD-A2) is bound with Asp75 (in Rnd1) through sidechain interaction for 73% of the time. Gln100 (in RBD-A2) and Asn76 (in Rnd1) form contacts for 90% of time. In the HSP state, Arg92 and Asn76 make contact up to 85% of the time, while HSP98 and Asp75 form contact for up to 79% of time.

For the complex of RBD-B1 with Rnd1, RBD residues from residue 67 to 100 including the L3 loop, β4, L4 loop, α2 helix, and β5 strand are at the binding interface in the HSD form; while RES69 to RES100 are on the binding interface in the HSP form. As noted above, there are two

HSD/HSP residues on RBD-B1, HSP74 and HSP98, both at the the binding interface. For Rac1, mostly β2 and β3, and α3 are at the binding interface. But in the HSD form, part of α2 is also at the binding interface. In the HSD form, Ala72 (on RBD-B1) and Glu48 (on Rnd1) form contacts for around 60% of time, while HSP98 and Asn76 form contact for around 54% of time; HSD74 and Trp66 form contacts for up to 33% of time; Lys100 and Tyr73 form contact for around 30% of time. In the HSP state, HSP74 in RBD-B1 forms hydrogen bonds with Asn49 sidechain for 94% of the time. Lys100 mainchain forms hydrogen bonds with Asp75 sidechain for 50% of the time, and with the Asn76 sidechain for 57% of the time. The Ser69 sidechain on RBD-B1 forms hydrogen bond with the Tyr74 sidechain for 32% of the time. Again, some of these contacts are seen in the orginal crystal structure, but due to the fluctuations at the interface, the overall contact time is always less than 100%, giving additional contacts compared to the static structures.

For the RBD-B1 : Rac1 complex in the HSD form (Table S4), the binding interface residues are from residue 68 to 106, which includes the L3 loop, β-strand 4, L4 loop, α-helix 2, and β-strand 5. For the complex in the HSP form(Table S5), the binding interface residues range from residue 73 to 114. So the L3 loop contributes to the HSD state, while the β-strand 5 contributes to binding in the HSP state. There are in total two protonated His (HSP) residues in RBD-B1. One is HSP74, the other is HSP98. Both of them contributed to the binding in the HSP state (Table S5). For the Rac1, mostly β2, β3, and α2 regions comprise the binding interface with RBDs in the HSD state. In the HSP form, mostly β2 and α2, but part of β1 and α3 are also at the binding interface. Focusing on the residue pairs that form the most persistent contacts in the HSD state, Asp81 side chain (on RBD-B1) and Arg66 sidechain (on Rac1) form contact for 72% of the simulation time, while up to 42% of time His98 and Lys100 (on RBD-B1) are bound with Arg66 and Asp63/Tyr64 (on Rac1). In the HSP state, up to 54% of time Gly73 (on RBD-B1) and Asp38 (on Rac1) are in contact; while other regions on the binding interface are explored more briefly. There are two HSP residues in the Rac1 GTPase. One is HSP103, and the other is HSP104. They did not contribute significantly to the binding.

For the RBD-A1 : Rac1 complexes, the binding interface residues are very consistent (Table S6 and S7 for HSD and HSP states respectively). Counting the residue pairs forming contacts with an occupancy greater than 5%, the binding interface, residues from residues 69 to 100 contribute to the binding for both the HSD and HSP states, which are the L3 loop, β4, L4 loop and α2 region. There are two HSP residues at pH 6.0 in the RBD-A1 protein: one is HSP21, while the other is HSP98. The second HSP contributed to the binding, mainly to Arg66 of Rac1 [29% in RBD-B1 Rac1 vs. 39% in RBD-A1 Rac1]. For Rac1, mostly β2 and β3, and α2 are on the binding interface. In the HSP form, α3 is also at the binding interface. Rac1 HSP103 and HSP104, again are not at the close-contact binding interface, but similarly to the RBD-B1 : Rac1 complex, one of these histidines features in contacts with an RBD Asp (65% HSP103 with Asp87 in RBD-A1:Rac1 vs. 13% HSP104 with Asp81 in RBD-B1:Rac1). Many of the details of contacts at the binding interface differ between RBD-A1 and –B1. In the HSD state, Arg73 (on RBD-A1) makes contact with Asp74 (on Rac1) in 36% of the simulation time; Arg92 (on RBD-A1) makes contact with Glu62 (on Rac1) for 27% of time. In the HSP form, Asn94 forms contacts with Arg66 (on Rac1) for 87% of time.

2. Supplementary **Figures:**

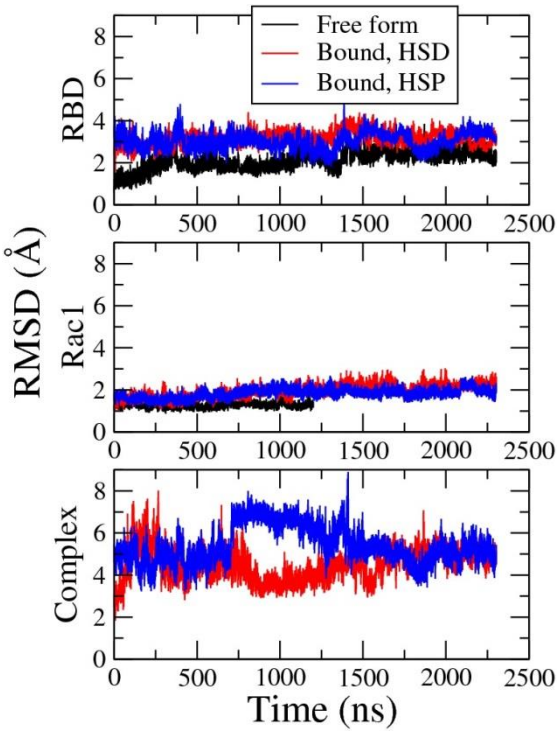

Figure S1. RMSD for (top) plexinB1 RBD in the free and bound forms, (mid.) Rac1 GTPase in the free and bound forms, and (bot.) the RMSD for the entire RBD-B1 : Rac1 complex in the two His-protonation states.
As can be seen, the simulations only show modest fluctuations around the average RMSD values by 500-750 ns for the free proteins and for the internal dynamics/domain level fluctuations of the bound proteins. For this particular simulation, the orientation/distance of the proteins in the complex undergoes a larger transition at 750 ns, lasting to approx. 1500 ns and a longer trajectory of 2.4 μs was run. It should be noted that this transition arises because the RBD-B1 free structure was taken from the RBD-B1 : Rnd1 crystal structure (2REX) where this region binds back to the RBD – an interaction that was thought to be a crystal artefact, but this interaction remains stable in the free protein simulation started from this structure. By contrast, the RBD-B1: Rac1 interface was derived from a different crystal form (3SU8), yet the L1 loop region was also modeled initially in a bound back state. In the HSD simulations L1 moves considerably away and is slightly more flexible, while in the simulations with charged His, the loop detaches completely (both in complexes with Rac1 and especially with Rnd1) and is substantially flexible.

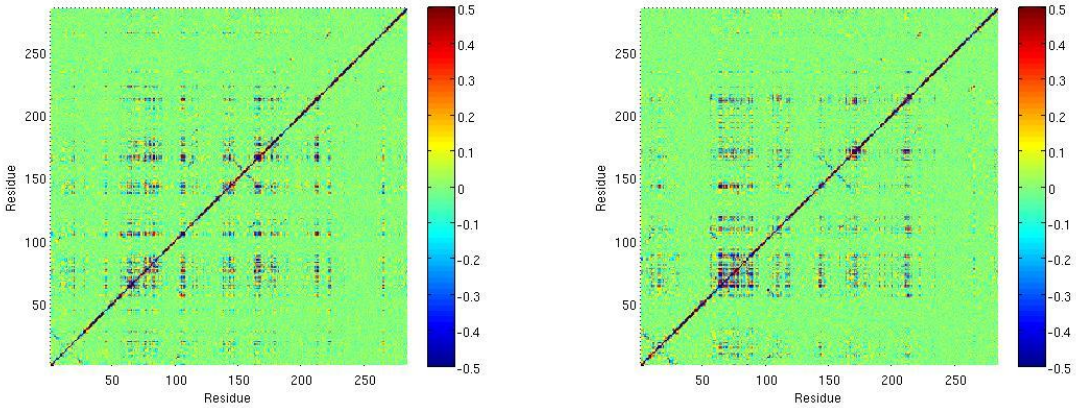

Figure S2. Dihedral angle covariance matrix for plexinB1 RBD bound with Rac1 GTPase in the HSD (Left) and HSP (right) state.

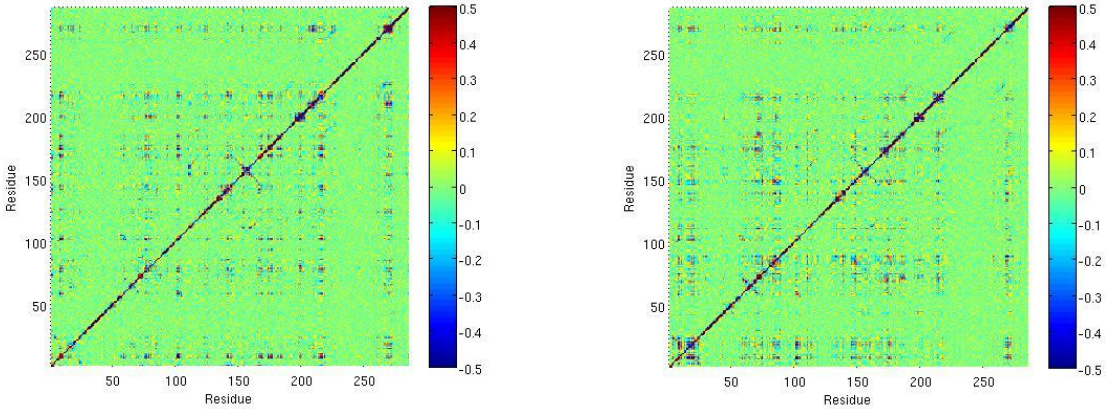

Figure S3. Dihedral angle covariance matrix for plexinB1 RBD bound with Rnd1 GTPase in the HSD (Left) and HSP (right) state.

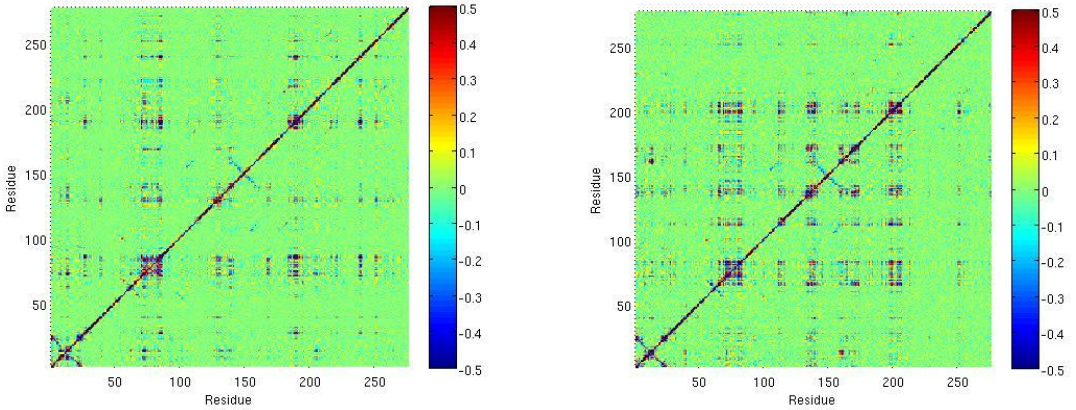

Figure S4. Dihedral angle covariance matrix for plexinA1 RBD bound with Rac1 GTPase in the HSD (Left) and HSP (right) state.

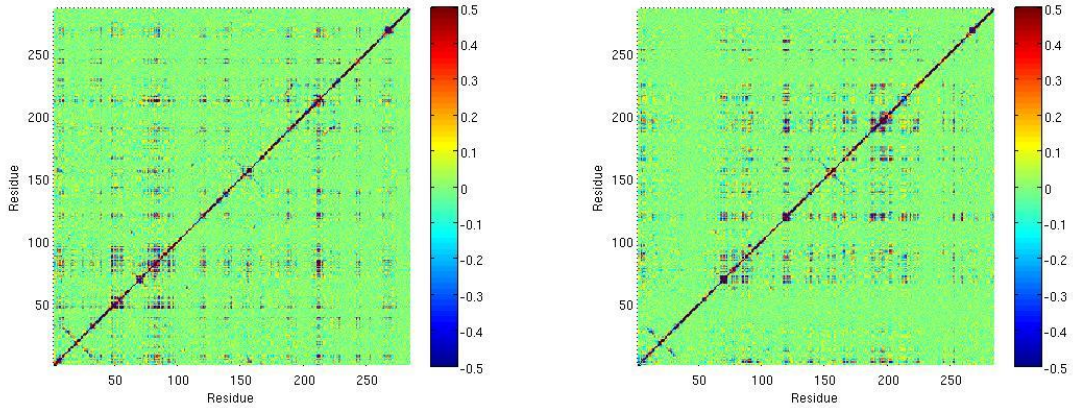

Figure S5. Dihedral angle covariance matrix for plexinA2 RBD bound with Rnd1 GTPase in the HSD (Left) and HSP (right) state.

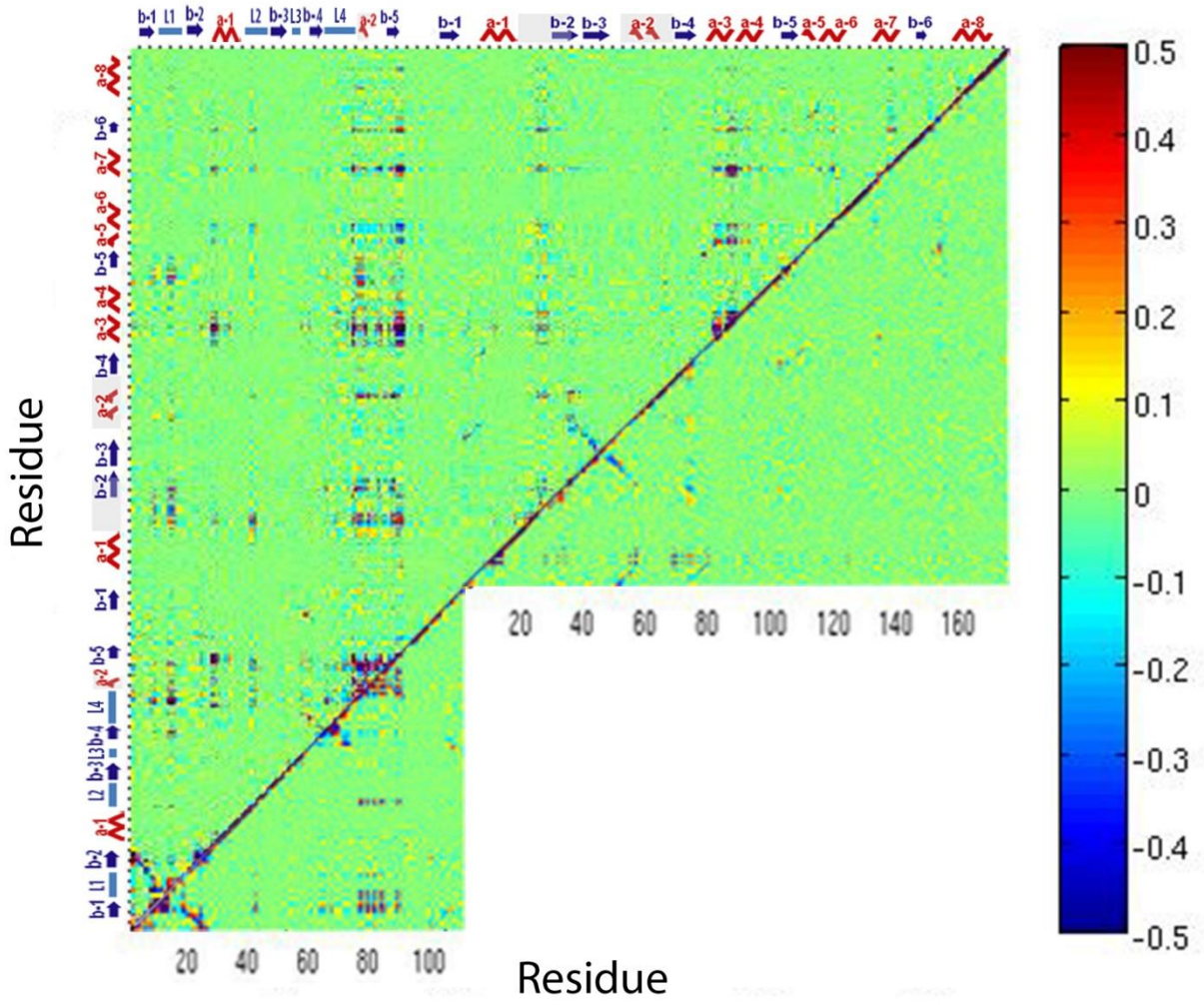

Figure S6. Dihedral angle covariance matrix comparison for plexinA1 RBD bound with Rac1 GTPase in HSD state (above diagonal), plexinA1 RBD free state (left, below diagonal) and Rac1 GTPase in free form (right, below diagonal).

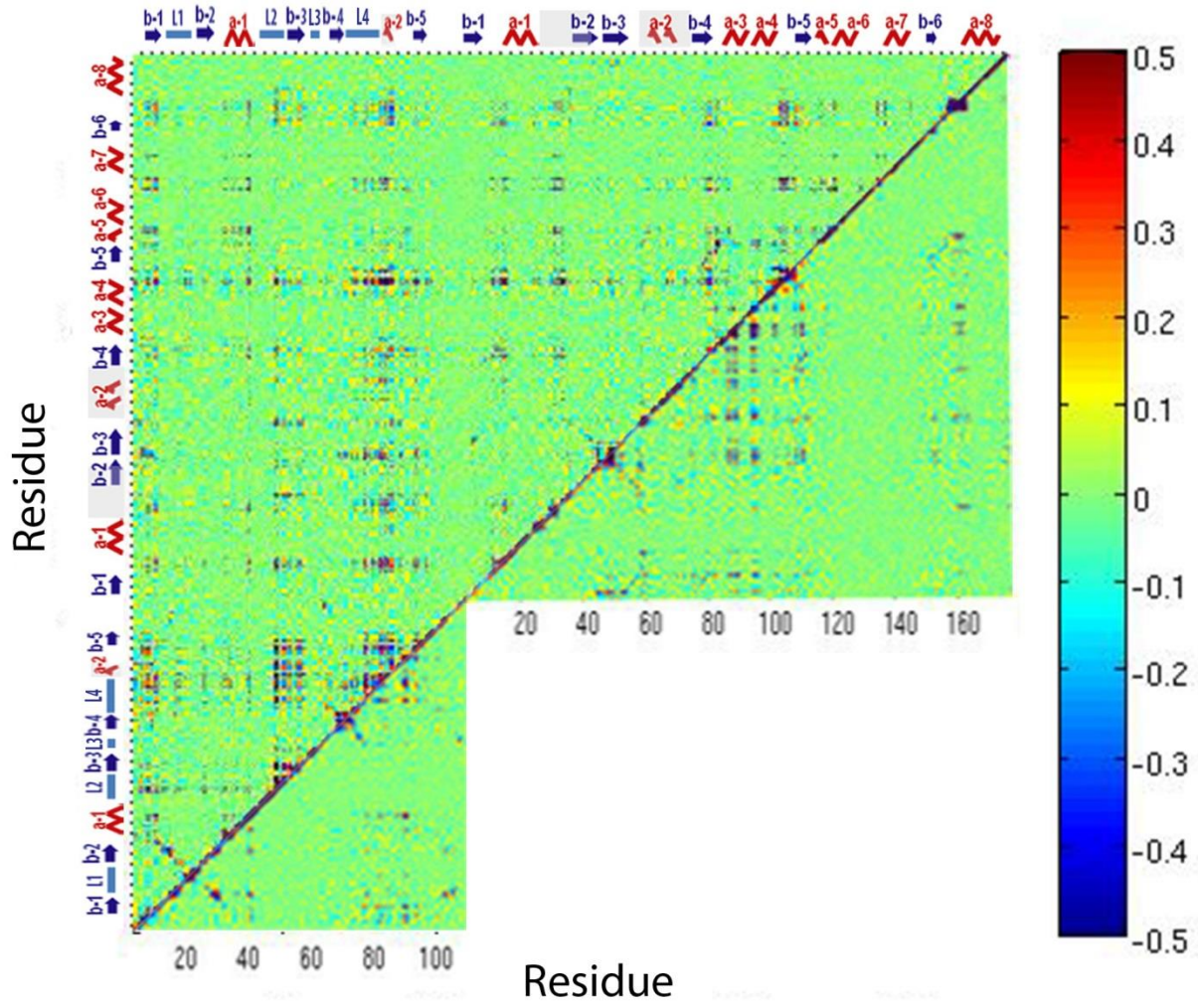

Figure S7. Dihedral angle covariance matrix comparison for plexinA2 RBD bound with Rnd1 GTPase in the HSD (above diagonal) , plexinA2 RBD in free form, and Rnd1 GTPase in free form. The numbering of residues is consistent with the sequence alignment and numbering shown in the supplemental materials.

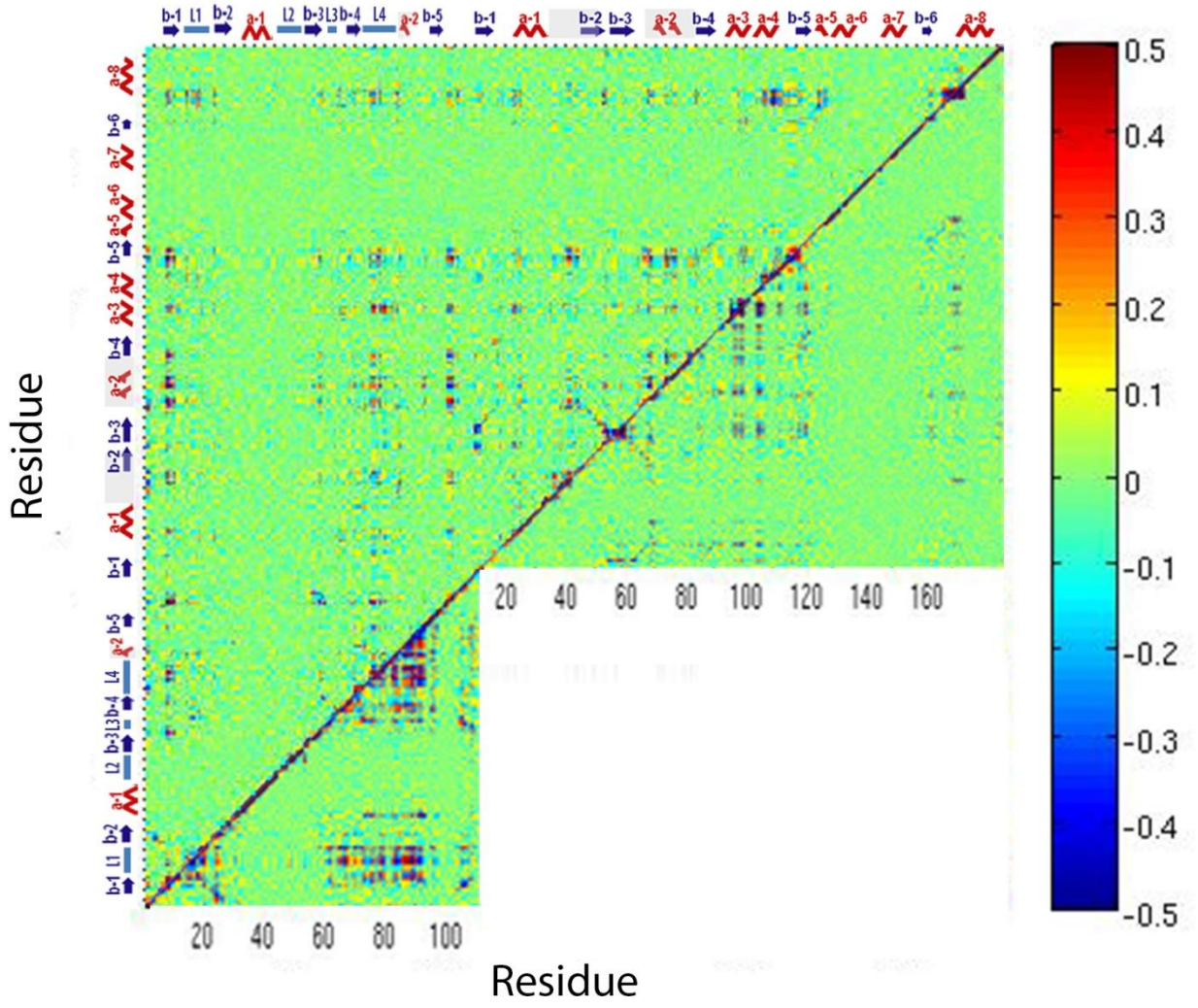

Figure S8. Dihedral angle covariance matrix comparison for plexinB1 RBD bound with Rnd1 GTPase in HSD state (above diagonal), plexinB1 RBD free state (below diagonal, left) and Rnd1 GTPase in free form (above diagonal, right).

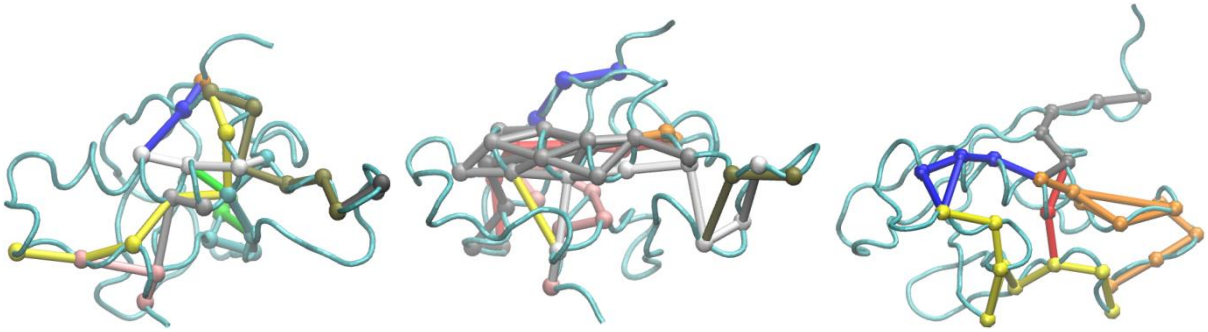

Figure S9. Optimized signaling pathways indicated for free RBD domains of plexinB1(Left), plexinA1 (Middle),and plexinA2 (Right). Different colors represent the signal pathways between the most highly correlated residue pairs. PlexinB1 and plexinA1 RBD domains have more connectivities than plexinA2 RBD, which is consistent with critical nodes results (not shown).

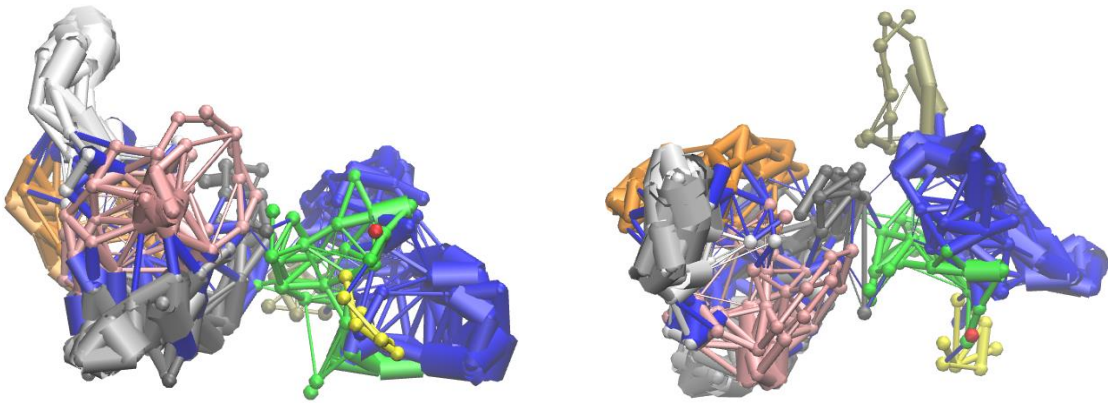

Figure S10 (a). PlexinB1 bound with Rac1 GTPase (both in protonated state) in sideview (Left) and topview (Right) showing a dynamical network analysis results comparison: (left) bound form of the network structure oriented in the same direction as in Fig. 6 (a) ; (right) bound form network structure rotated 90 degrees around the long/x-axis.

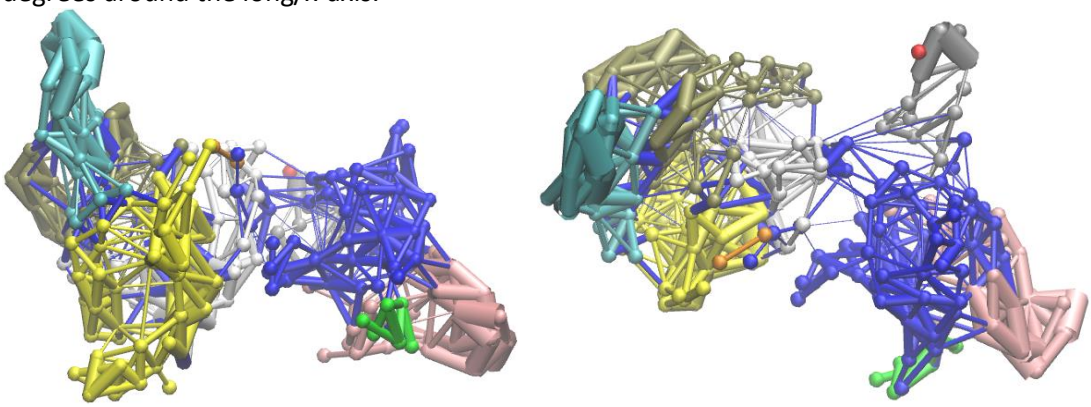

Figure S10 (b). Plexin-A1 bound with Rac1 GTPase (both in protonated state) in sideview (Left) and topview (Right) showing a dynamical network analysis results comparison: (left) bound form of the network structure oriented as above ; (right) bound form network structure rotated 90 degrees around the long/x-axis.

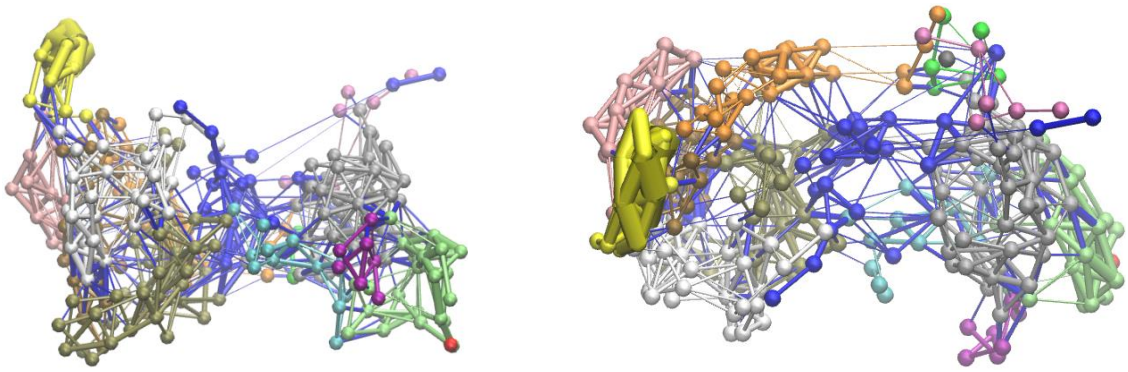

Figure S10 (c). Plexin-A2 bound with Rnd1 GTPase (both in protonated state) in sideview (Left) and topview (Right) showing a dynamical network analysis results comparison: (left) bound form of the network structure oriented as above; (right) bound form network structure rotated 90 degrees around the long/x-axis.

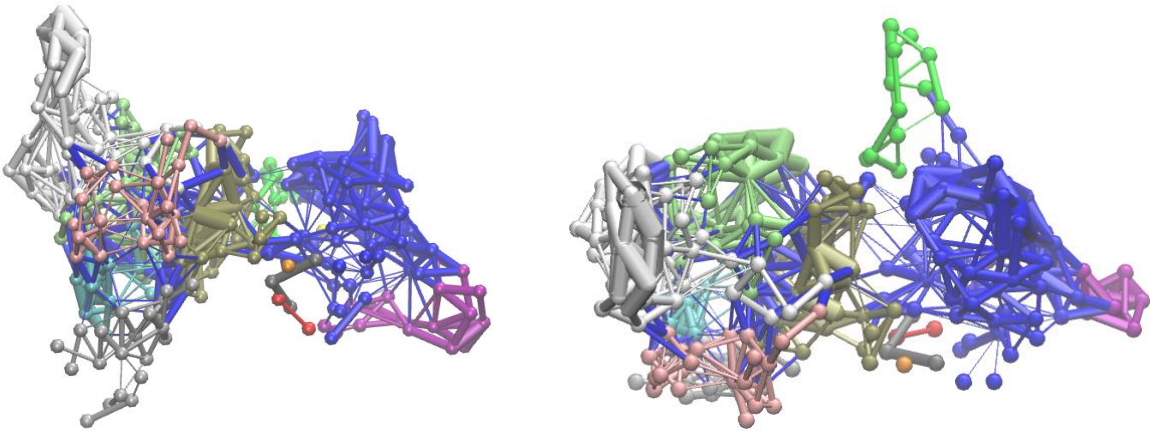

Figure S10 (d). Plexin-B1 bound with Rnd1 GTPase (both in protonated state) in sideview (Left) and topview (Right) showing a dynamical network analysis results comparison: (left) bound form of the network structure oriented in the same direction as above; (right) bound form network structure rotated 90 degrees around the long/x-axis.

No obvious difference in dynamic network was observed for complexes in deprotonated state (Fig. 6) or in protonated state (here) for most complexes. However, in case of the protonated RBD-B1 Rac1 complex (a) there are 2-3 weak interprotein connections linking networks. The RBD-A1 and Rac1 GTPase in HSP state (b) shows hints of across the interface -communication compared to HSD state.

Detailed Analysis of protein-protein contacts:

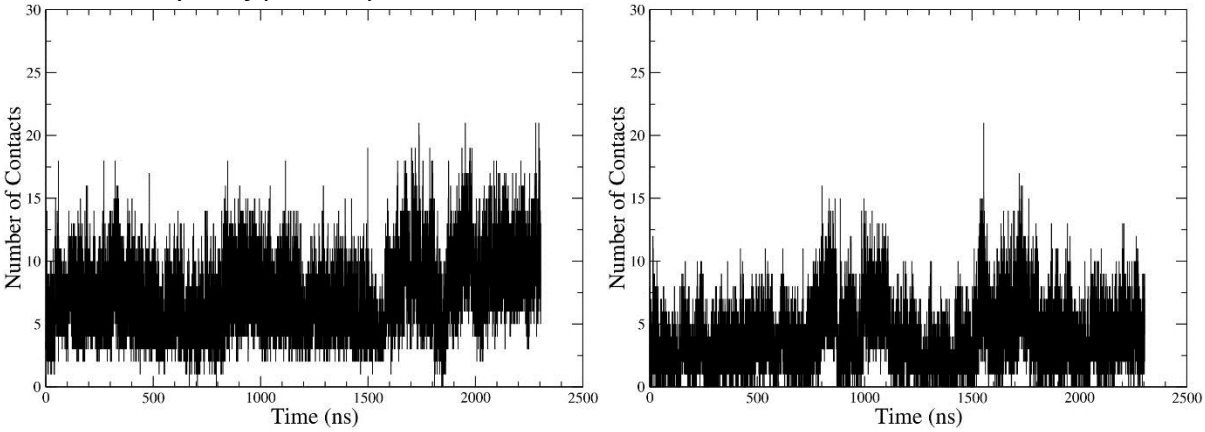

Figure S11(a). Number of contacts for RBD-B1 and Rac1 GTPase complexes in (a) the HSD state and (b) the HSP state over the time-course of the 2.4 μs simulations.

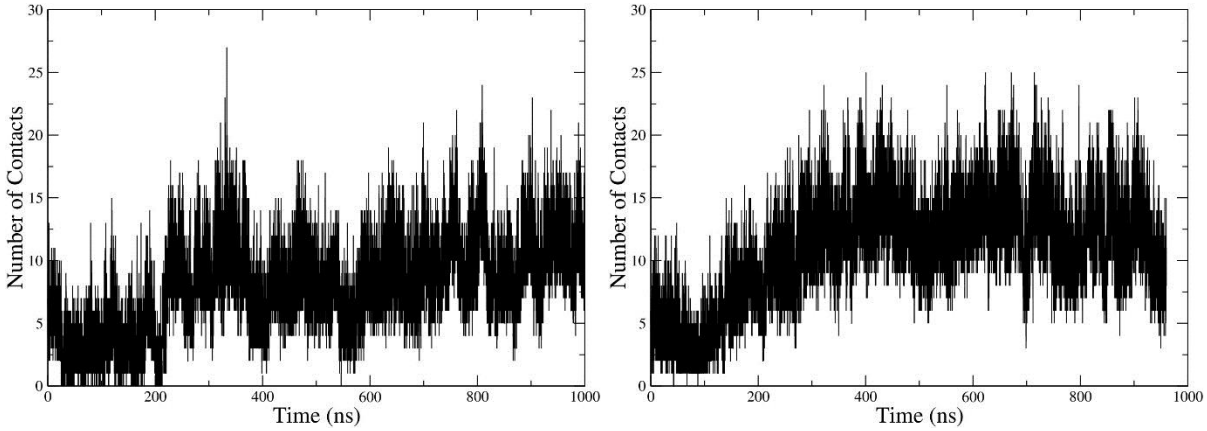

Figure S11 (b). Number of contacts for RBD-A1 and Rac1 GTPase in the HSD state (Left) and the HSP state (Right) during 1.0 μs of simulation.

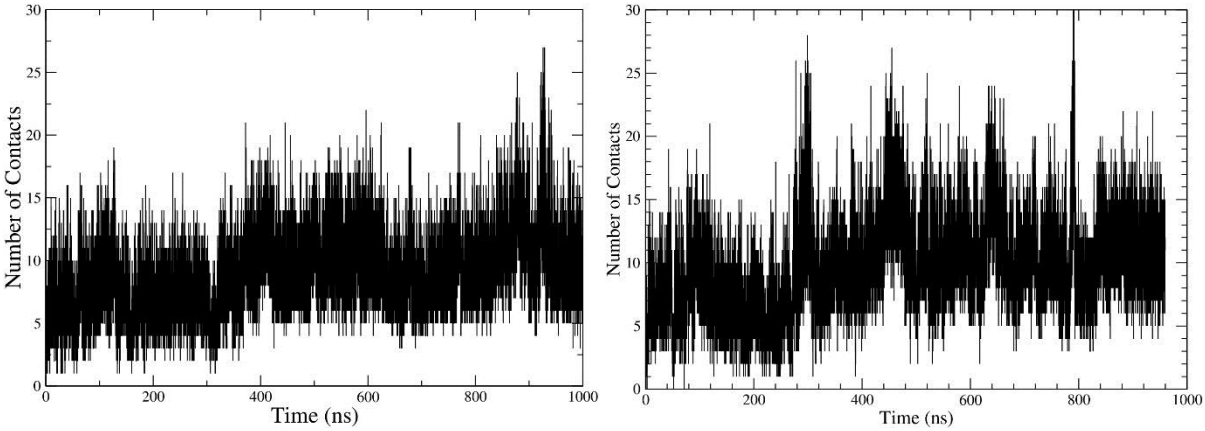

Figure S11 (c). Number of contacts for RBD-A2 and Rnd1 GTPase in HSD state (Left) and HSP state (Right) during 1.0 us simulations.

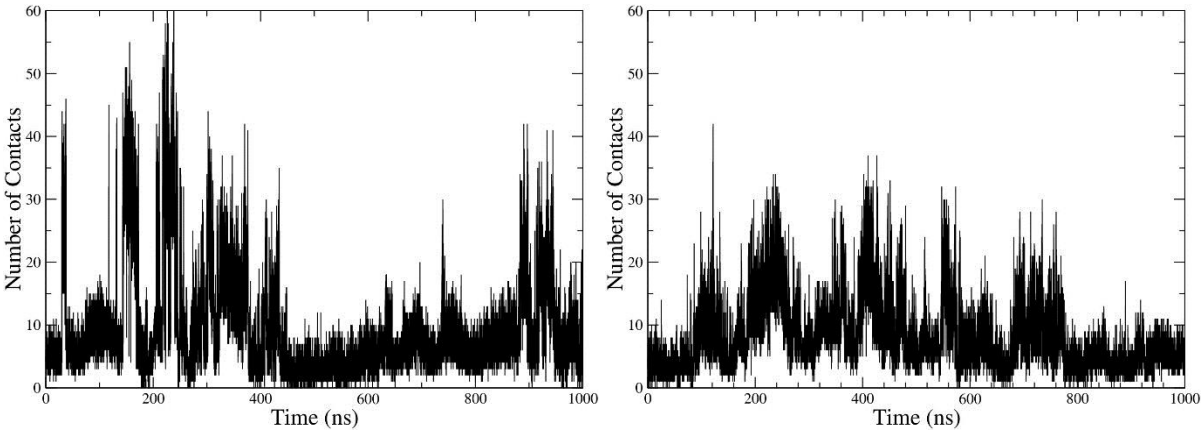

Figure S11 (d). Number of contacts for RBD-B1 and Rnd1 GTPase in HSD state (Left) and HSP state (Right) during 1.0 us simulations.

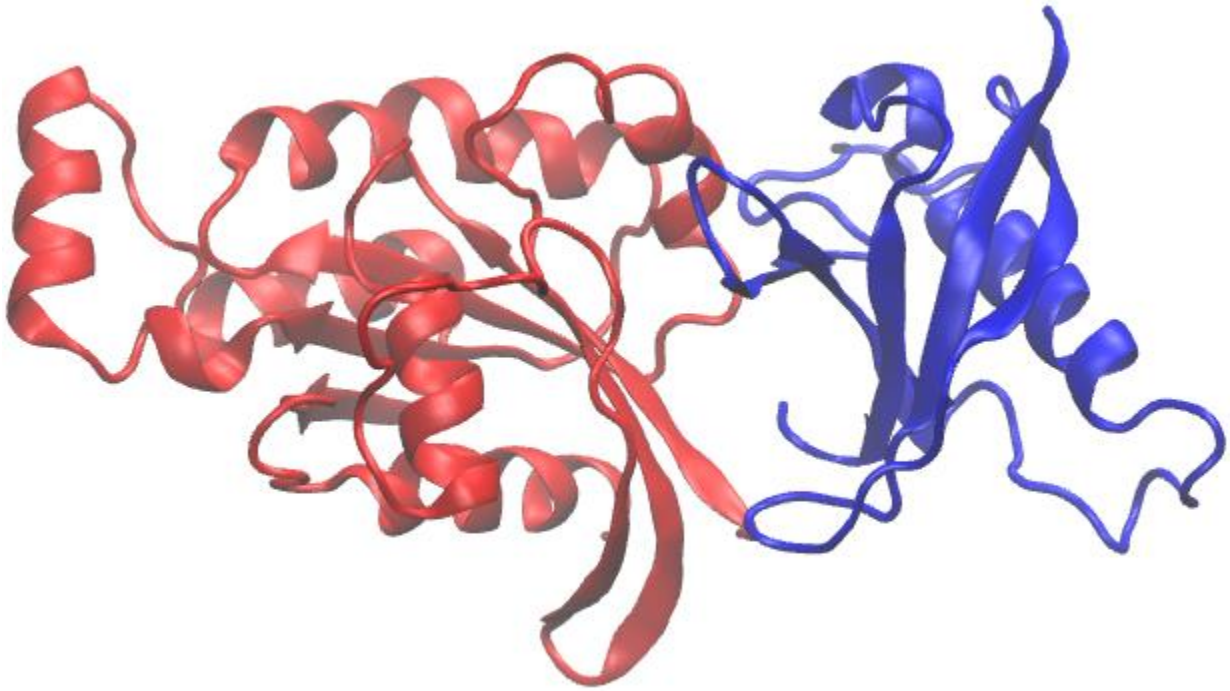

Figure S12. The complex structure of RBD-B1 & Rac1 in protonated state at around 750 ns during 2.4 μs all atom molecular dynamics simulations. The Rac1 is shown in red (left) and RBD-B1 in blue (right). The alignment of the complex is similar to Figure1 in the main text.

3. Additional **Materials and Methods:**

Dihedral Angle Correlation Calculation. To quantitatively describe the motional correlations of the backbone, we calculated the ϕ and φ cross-correlation matrices. ϕ describes the rotation around the N−Cα bond and involves the C−N−Cα−C group of atoms. φ describes the rotation around the Cα -C' bond and involves the N−Cα−C'−N atoms. Both ϕ and φ are calculated for all residues except for the N- and C-termini using the CHARMM program.

Because both ϕ and φ are angular variables, to avoid the periodicity problem, the circular correlation coefficient, which has a T-linear dependence, was calculated in this project –as in our previous paper [1]- following the method of Fisher [2, 3] and Mardia and Jupp.[4]. The circular correlation matrix element r_T for two circular variables x and y can be calculated with eqs (1−9) during the simulation time i from 1 to N:

$$\mathrm{r_T} = \frac{4(\mathrm{AB} - \mathrm{CD})}{\sqrt{(N^2 - \mathrm{E}^2 - \mathrm{F}^2)(N^2 - G^2 - H^2)}} \qquad (1)$$

Where:

$$A = \sum \cos(x_i)\cos(y_i) \qquad (2)$$

$$B = \sum \sin(x_i)\sin(y_i) \qquad (3)$$

$$C = \sum \cos(x_i)\sin(y_i) \qquad (4)$$

$$D = \sum \sin(x_i)\cos(y_i) \qquad (5)$$

$$E = \sum \cos(2x_i) \qquad (6)$$

$$F = \sum \sin(2x_i) \qquad (7)$$

$$G = \sum \cos(2y_i) \qquad (8)$$

$$H = \sum \sin(2y_i) \qquad (9)$$

Here, N is no less than 22000 coordinate frames (typically the final 500 ns of each trajectory with an output frequency of 48 ps), so the above T-linear association has a good enough sampling. x and y are ϕ or φ in radians. The ϕ−φ cross-correlation coefficients (matrices) were calculated of all combinations of dihedral angles. In order to simplify the data representation, we combined the ϕ−ϕ, ϕ−φ, and φ−φ correlation matrices and always chose the element with the largest magnitude at residue pair position to build the final matrix.

4. Movies

750ns-rmsd-change-movie2.mpg

For plexin-B1 RBD bound with Rac1 GTPase (both in the protonated state), a movie was made to show the binding interface between the proteins during the 2.4 μs all atom molecular dynamics simulation. It was found that at around 750 ns, the L1 loop of plexin-B1 RBD stretched to reach the Rac1 GTPase and that this caused a significant structure deviation of the complex from the original structure, thus a sharp increase of the complex RMSD was observed. The plexin-B1 RBD was shown in blue, while Rac1 was shown in red. The

complex was aligned in the same orientation as Figure 1 in the main context. However, this is the only larger scale perturbation we observed and it should be noted that the structure relaxes back to near the starting structure towards the end of the trajectory (see also Fig. S1).

Additional References:

1. Zhang, L.; Centa, T.; Buck, M. Structure and Dynamics Analysis on Plexin-B1 Rho-GTPase Binding Domain Monomer and Dimer. *J. Phys. Chem. B.* **2014**, 118(26), 7302-11.
2. Fisher, N. I.; Lee, A. J. A Correlation Coefficient for Circular Data. *Biometrika* **1983**, 70, 327−332.
3. Fisher, N. I. Statistical Analysis of Circular Data; Cambridge University Press: New York, **1993**, p 277.
4. Mardia, K. V.; Jupp, P. E. Directional Statistics; Wiley: Chichester, UK, **2000**, p 429.